

Chemical Abundances in the Nuclear Star Cluster of the Milky Way: α -Element Trends and Their Similarities with the Inner Bulge

N. Ryde, G. Nandakumar, M. Schultheis, G. Kordopatis, P. di Matteo, M. Haywood, R. Schödel, F. Nogueras-Lara, R. M. Rich, B. Thorsbro, G. Mace, O. Agertz, A. M. Amarsi, J. Kocher, M. Molero, L. Origlia, G. Pagnini, E. Spitoni

<https://arxiv.org/abs/2412.04528>

Abstract

A chemical characterization of the Galactic Center is essential for understanding its formation and structural evolution. Trends of α -elements, such as Mg, Si, and Ca, serve as powerful diagnostic tools, offering insights into star-formation rates and gas-infall history. However, high extinction has previously hindered such studies. In this study, we present a detailed chemical abundance analysis of M giants in the Milky Way's Nuclear Star Cluster (NSC), focusing on α -element trends with metallicity. High-resolution, near-infrared spectra were obtained using the IGRINS spectrograph on the Gemini South telescope for nine M giants. Careful selection of spectral lines, based on a solar-neighborhood control sample of 50 M giants, was implemented to minimize systematic uncertainties. Our findings show enhanced α -element abundances in the predominantly metal-rich NSC stars, consistent with trends in the inner bulge. The NSC stars follow the high- $[\alpha/\text{Fe}]$ envelope seen in the solar vicinity's metal-rich population, indicating a high star-formation rate. The α -element trends decrease with increasing metallicity, also at the highest metallicities. Our results suggest the NSC population likely shares a similar evolutionary history with the inner bulge, challenging the idea of a recent dominant star formation burst. This connection between the NSC and the inner-disk sequence suggests that the chemical properties of extragalactic NSCs of Milky Way type galaxies could serve as a proxy for understanding the host galaxies' evolutionary processes.

1. Introduction

- For a holistic picture of the Galactic Center region, a chemical characterization of this region is a critical component.
 - Trends of α -elements, such as Mg, Si, and Ca, serve as powerful **diagnostic tools**, offering insights into star-formation rates and gas-infall history.
- The center of the Milky Way consists of
 - NSC (Nuclear Star Cluster)** ← this paper
 - a half-light radius of ~ 4 pc, a diameter of ~ 12 pc, $\sim 2 \times 10^7$ Msun
 - NSD (Nuclear Stellar Disk)
 - CMZ (Central Molecular Zone)
- High extinction in the inner region
 - Useful for IR spectroscopy
- They investigated the abundance trends of the α elements as a function of metallicity for a sample of **stars in the NSC**, differentially against the trends from a control sample of **the same type of stars in the solar neighbourhood**.
 - Search for differences that may reflect a different chemical evolution in them.

2. Observation and Data Reduction

- Targets : 9 NSC M giants ($T_{\text{eff}} < 4000$ K)
- Instrument: Gemini South/IGRINS
 - $R \sim 45000$
 - H + Ks bands (1.45-2.5 μm)
- Observation period :
 - May 2022- Apr 2024
- Control samples are from Nandakumar et al. (2023) and Nandakumar et al. (2024 b)
 - Observed by the same instrument.

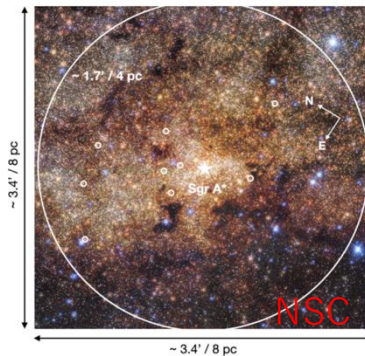


Figure 2. Colour-magnitude diagram, K versus H-K, of the NSC (Nishiyama et al. 2013) with our observed targets indicated by red circles.

3. Analysis

Confirmation of NGC stars

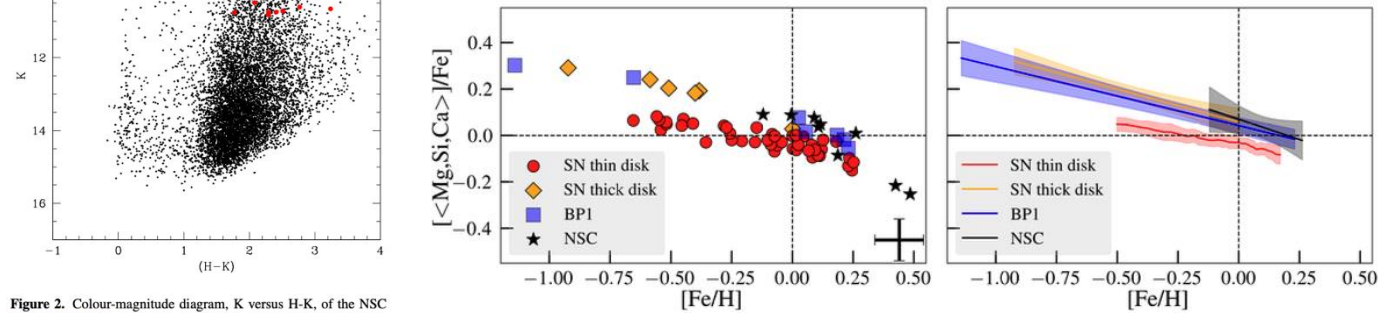
- Radial velocity + proper motion
 - orbit model by AGAMA package confined to NSC
- Red colors : $H - K > 1.8$ mag (Figure.2)
 - High extinction typical of NSC
- Diffuse Interstellar Band (DIB) at $\lambda \sim 1.527 \mu\text{m}$
 - DIB = ISM absorption → correlates with extinction → $A_v \sim 20$ -25 mag \sim typical for NSC region

Spectral synthesis

- Spectral synthesis method
 - The synthetic spectrum is generated by SME tool (Valenti & Piskunov 1996, 2012), assuming atmosphere model of MARCS (Gustafsson et al. 2008)
 - Lines:
 - Adopt vetted M-giant line list (Nandakumar+) + add 2 Si lines in K band (21368.7 Å, 21874.2 Å)
- derive fundamental stellar parameters (T_{eff} , $\log g$, $[\text{Fe}/\text{H}]$, ξ_{micro})

4. Results

- The NSC $[\alpha/\text{Fe}]$ trend shows a clear and steady decrease with increasing metallicity.



SN thin/thick disk → 50 M giants in 太陽近傍の銀河円盤領域
BP 1 → Inner bulge ($b \approx +1^\circ$ field) from Nandakumar et al. 2024b

5. Discussion

- CCSNe (fast) → α elements
- SNe Ia (delayed) → Fe
- $[\alpha/\text{Fe}]$ traces enrichment timescale
- Bule** (Inner bulge) and **black** (NSC) lines are similar.
 - High $[\alpha/\text{Fe}]$ at high $[\text{Fe}/\text{H}]$
 - predominately rapid chemical enrichment, high SFR
- The chemical pattern observed in **the NSC stars** is consistent with that seen in solar vicinity **thick-disk stars** at the same $[\text{Fe}/\text{H}]$ values, exhibiting similar levels of α -element enhancement.
 - "inner-disk sequence" like evolution
- NSC chemistry is similar to inner bulge one.
 - likely shared evolutionary history.
 - not dominated by a more recent, dominant burst of star formation proposed by Chen et al. 2023

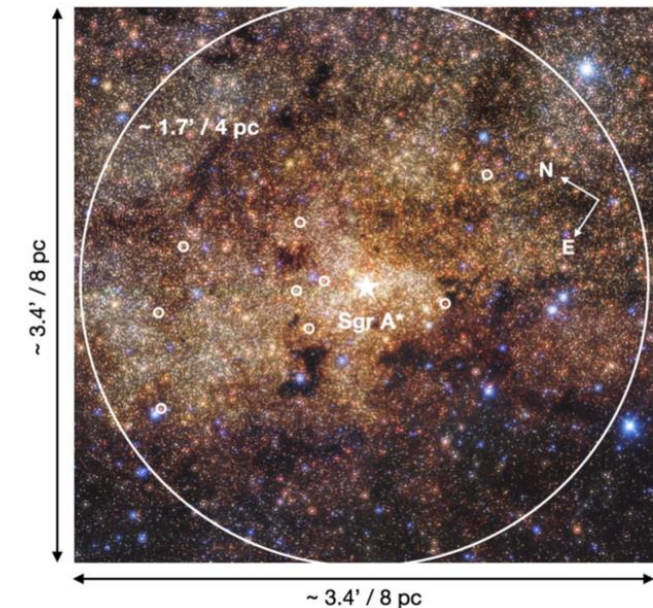


Figure 1. GALACTICNUCLEUS JHK_s image of the Milky Way's NSC (Nogueras-Lara et al. 2018, 2019) showing the 9 stars for which we have obtained spectra, marked by white small circles. The image scale is $8 \times 8 \text{ pc}^2$ and the large white circle indicates the effective radius of the NSC ($\sim 4 \text{ pc}$, or $\sim 100''$), while the position of the supermassive black hole, A*, is denoted by a white star in the middle of the image. The directions East (E) and North (N) are labeled in the upper right corner.

Table 1. Observational details of M giant stars.

Name ^a	RA	DEC	H ^b	K _s ^b	Date	Exp. Time	S/N _H / S/N _K ^c	id ^d	Telluric star
	h:m:s	d:m:s	[mag]	[mag]	UT	[s]	per res. element		AOV
FK48 ⁽²⁾	17:45:41.301	-29:00:08.406	12.53	10.76	2023-04-30	2240	35/105	48	HIP86098
FK5020265 ⁽²⁾	17:45:46.187	-28:59:48.253	11.84	9.91	2023-03-24	840	50/150	5020265	HIP86098
FK87 ⁽¹⁾	17:45:40.671	-29:00:15.318	13.04	10.75	2022-05-16	1620	45/175	87	HIP86098
Feld31 ⁽²⁾	17:45:42.000	-29:00:20.000	13.38	10.61	2023-04-26	1200	20/150	31	HIP86552
Feld84 ⁽²⁾	17:45:39.400	-29:00:58.900	13.90	10.66	2023-04-28	2080	10/135	84	HIP86098
GC15540 ⁽²⁾	17:45:41.900	-28:59:23.390	12.57	10.49	2023-03-24	2200	35/120	3001047	HIP86098
GC16890 ⁽²⁾	17:45:43.900	-28:59:28.500	13.23	10.72	2023-04-26	2240	20/105	3000179	HIP88152
GC13727 ⁽³⁾	17:45:39.590	-28:59:56.210	13.11	10.82	2024-04-11	2520	20/120	73	HIP94663
GC16895 ⁽³⁾	17:45:35.640	-29:00:47.000	13.16	10.75	2024-04-20	2400	20/115	1012095	HIP86098

^aGemini-S Programme identification: ⁽¹⁾ GS2022A-Q-208; ⁽²⁾ GS2023A-Q-304; ⁽³⁾ GS2024A-Q-304.

^bThe H and K magnitudes are from Nishiyama et al. (2013)

^cThe signal-to-noise ratios were provided by RRISA (The Raw & Reduced IGRINS Spectral Archive; Sawczynec et al. 2022) and are the average S/N for the H- and K-bands per resolution element. The S/N varies over the orders and is lowest at the ends of the orders.

^dIdentification number from Feldmeier-Krause et al. (2017a, 2020).

Table 2. Stellar and orbit parameters, and C, N, and O abundances for the NSC giants.

Star	T_{eff}	$\log g$	[Fe/H]	ξ_{micro}	[C/Fe]	[N/Fe]	[O/Fe] ^a	μ_l	μ_b	v_{los}	r_{apo}^b	z_{max}
	[K]	[log(cm s ⁻²)]	[dex]	[km s ⁻¹]	[dex]	[dex]	[dex]	[mas/yr]	[mas/yr]	[km s ⁻¹]	[pc]	[pc]
FK48	3440	0.6	0.12	1.8	0.12	0.25	0.09	-2.54	-0.42	0	9.81	6.70
FK5020265	3350	0.6	0.26	1.9	0.06	0.24	0.04	-3.94	5.71	157	9.93	8.47
FK87	3352	0.5	0.09	1.9	0.07	0.35	0.11	-	-	196	-	-
Feld31	3825	1.5	0.42	2.3	-0.04	0.5	-0.04	-1.02	3.25	118	10.32	7.29
Feld84	3709	1.4	0.48	2.7	0.03	0.47	-0.07	-	-	0	-	-
GC15540	3361	0.5	0.11	1.9	0.03	0.36	0.10	-2.68	2.57	0	8.17	6.21
GC16890	3423	0.7	0.19	2.0	0.02	0.33	0.06	-2.07	-1.30	236	8.85	7.02
GC13727	3356	0.4	0.00	2.1	0.20	0.32	0.16	0.74	-0.97	-59	9.17	6.76
GC16895	3366	0.4	-0.12	2.2	0.19	0.45	0.21	-7.93	0.33	-39	11.10	5.03

^aThe [O/Fe] is provided from a simple functional form of the [O/Fe] versus [Fe/H] trend in Nandakumar et al. (2023) based on the Amarsi et al. (2019) trend.

^b r_{apo} is the maximum apocentric radius from the galactic center projected on the x-y plane.

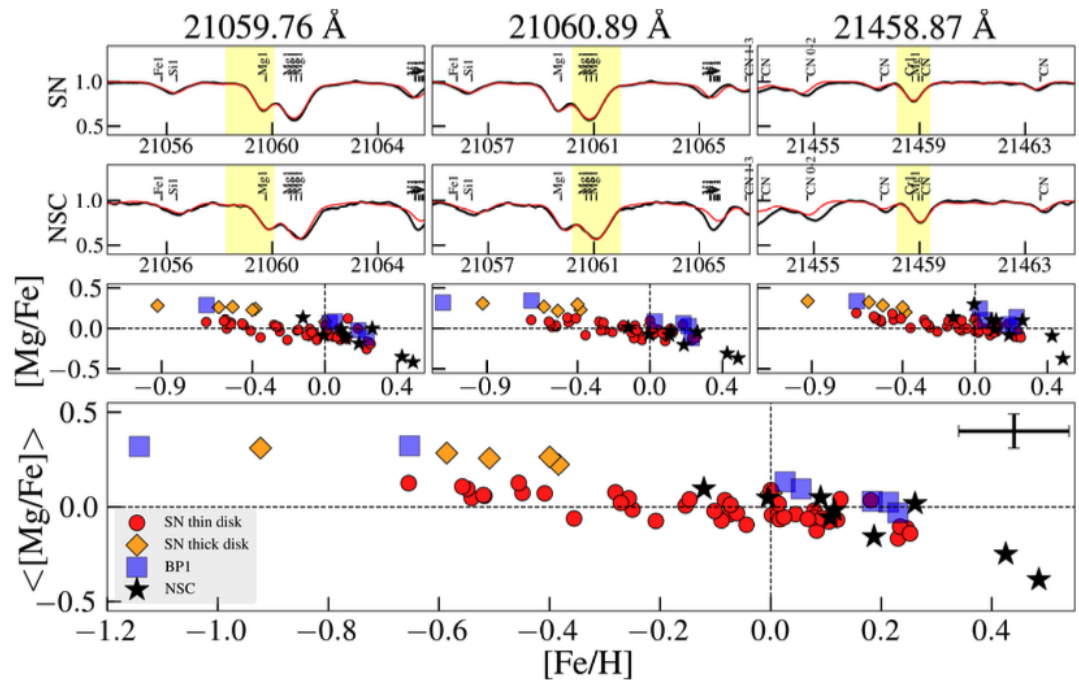


Figure 4. $[Mg/Fe]$ versus $[Fe/H]$ for different stellar populations. The Nuclear Star Cluster (NSC) stars are represented by black stars, the inner bulge stars from Nandakumar et al. (2024b) by blue squares, and the solar neighborhood thin-disk stars are depicted by red filled circles, while the thick-disk stars are shown as orange diamonds. In the upper two panels, the spectral lines used for the analysis are displayed, with a typical solar neighborhood star shown above and a typical NSC star (FK48) shown below. The trends derived from each individual spectral line are presented, along with the mean trend, which is displayed in the largest, bottom panel.

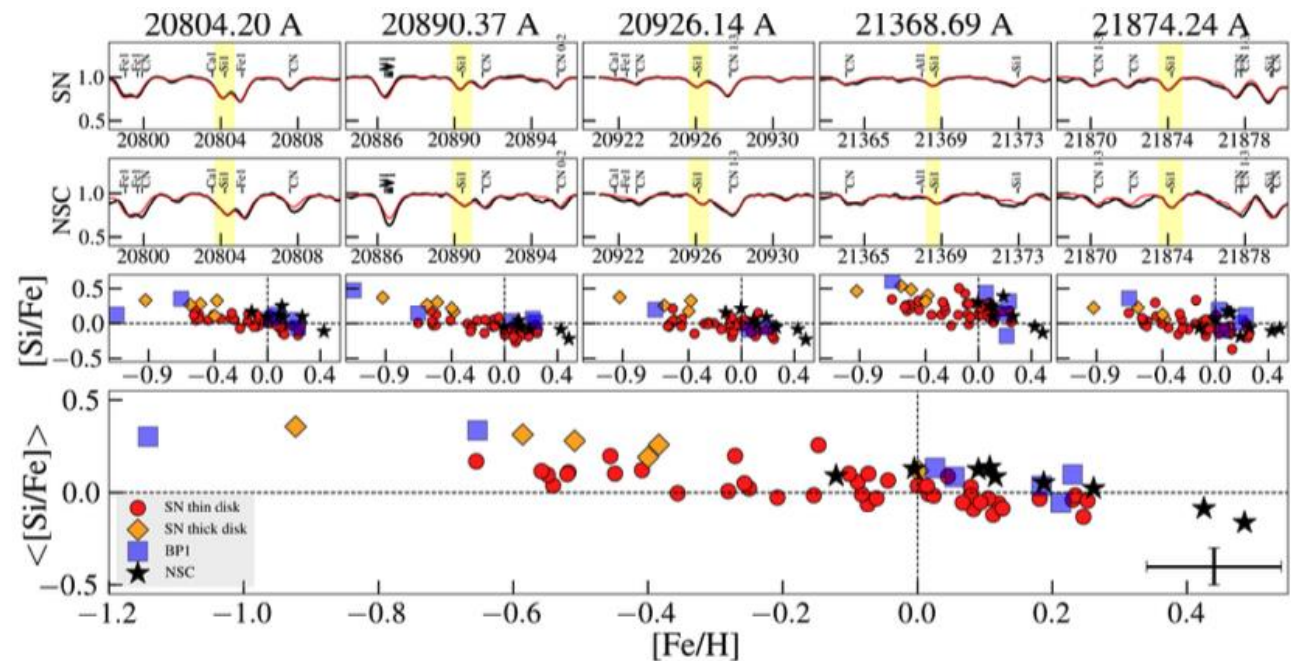


Figure 5. $[Si/Fe]$ versus $[Fe/H]$ for different stellar populations: NSC stars (black stars), inner bulge stars (blue squares), thin-disk stars (red circles), and thick-disk stars (orange diamonds). The upper panels display the spectral lines used, with a typical solar neighborhood star above and an NSC star (FK48) below. Trends from individual lines and the mean trend are shown in the bottom panel.

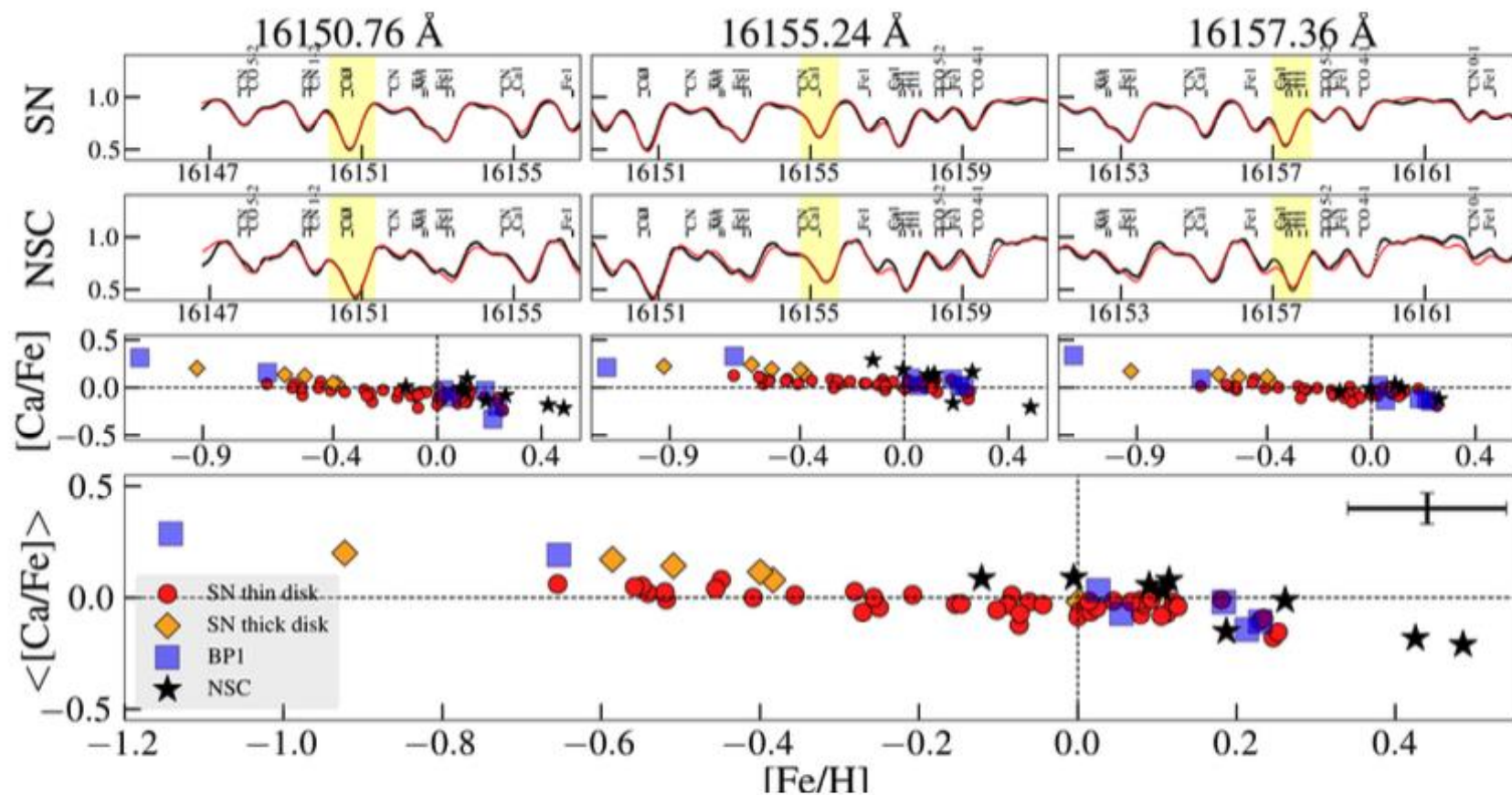


Figure 6. $[Ca/Fe]$ versus $[Fe/H]$ for different stellar populations: NSC stars (black stars), inner bulge stars (blue squares), thin-disk stars (red circles), and thick-disk stars (orange diamonds). The upper panels display the spectral lines used, with a typical solar neighborhood star above and an NSC star (FK48) below. Trends from individual three lines and the mean $[Ca/Fe]$ trend versus metallicity are shown in the bottom panels.